

Thrust Characteristics of a Laser-Assisted Pulsed Plasma Thruster

Masatoshi Kawakami*, Hideyuki Horisawa*, and Itsuro Kimura#

*Department of Aeronautics and Astronautics, Tokai University, 1117 Kitakaname, Hiratsuka, Kanagawa, 259-1292 JAPAN#Professor emeritus, University of Tokyo, 7-3-1 Hongo, Bunkyo-ku, Tokyo, 113-8856 JAPAN

Keywords: Laser propulsion, PPT, Laser-electric hybrid propulsion, ICCD camera observation, Torsion-balance thrust measurement.

Abstract

An assessment of a novel laser-electric hybrid propulsion system was conducted, in which a laser-induced plasma was induced through laser beam irradiation onto a solid target and accelerated by electrical means instead of direct acceleration only by using a laser beam. A fundamental study of newly developed rectangular laser-assisted pulsed-plasma thruster (PPT) was conducted. On discharge characteristics and thrust performances with increased peak current compared to our previous study to increase effects of electromagnetic forces on plasma acceleration. Maximum peak current increased for our early study by increasing electromagnetic effects in a laser assisted PPT. At 8.65 J discharge energy, the maximum current reached about 8000 A. Plasma behaviors emitted from a thruster in various cases were observed with an ICCD camera. It was shown that the plasma behaviors were almost identical between low and high voltage cases in initial several hundred nanoseconds, however, plasma emission with longer duration was observed in higher voltage cases. Canted current sheet structures were also observed in the higher voltage cases using a larger capacitor. With a newly developed torsion-balance type thrust stand, thrust performances of laser assisted PPT could be estimated. The impulse bit and specific impulse linearly increased. On the other hand, coupling coefficient and the thrust efficiency did not increase linearly. The coupling coefficient decreased with energy showing maximum value (20.8 μ Nsec/J) at 0 J, or in a pure laser ablation cases. Thrust efficiency first decreased with energy from 0 to 1.4 J and then increased linearly with energy from 1.4 J to 8.6 J. At 8.65 J operation, impulse bit of 38.1 μ Nsec, specific impulse of 3791 sec, thrust efficiency of 8 %, and coupling coefficient of 4.3 μ Nsec/J were obtained.

1. Introduction

Pulsed-plasma thrusters, PPTs, utilizing a solid propellant usually PTFE (Teflon), have attracted a growing interest for their system simplicity and advantages on miniaturization and mass reduction for the use of attitude or orbit control thrusters for small-sized spacecrafts, despite their low efficiency¹⁻⁴⁾. In their operations, short pulse discharges with several-microsecond duration are induced across an exposed propellant surface between electrodes, vaporizing and ionizing the surface, and also inducing a pressure force. Then an interaction of the discharge current

(tens of kA) and its self-induced magnetic field results as the electromagnetic force, or Lorentz force, acting on the plasma and inducing a directed plasma beam exhaust, or thrust. In this electromagnetic acceleration process, it is necessary to complete phase changes of the propellant, such as vaporization and ionization, and the electromagnetic acceleration at the same time within a short duration of a pulse discharge. Improvements of the thrust performance can be expected with shorter pulse duration cases, since it is capable of higher current per unit time or higher power input, namely higher thrust, and of reducing loads on electrodes. However, it is difficult to complete the process including the phase changes and electromagnetic acceleration simultaneously during the discharge pulse, because there is a delay in the phase change of the solid-propellant after the pulse discharge initiation. The surface of the propellant will continue to evaporate long after completion of the discharge pulse, providing mass that cannot experience acceleration to high speeds by the electromagnetic and gasdynamic forces. The various masses including low-speed macroparticles can have quite different velocities. Since the residual vapor or plasma from the late-time evaporation of the propellant surface remains in the discharge chamber due to the delay after the pulse discharge completion, which cannot contribute significantly to the impulse bit, it has been difficult for the thruster of this type to improve this mass loss of the propellant and thrust efficiency¹⁻⁴⁾.

In order to reduce this late-time ablation and to improve thrust efficiency, effects of the utilization of laser-pulse irradiation, or assistance, were studied, which can be expected to induce plasma from a solid-propellant surface in a short duration, i.e., using a short-duration conductive region of the plasma between electrodes, short-pulse switching or discharge can be achieved⁵⁻⁶⁾. Since the use of a shorter pulse of the laser enables a shorter duration of a pulsed-plasma in this case, a higher peak current and significant improvement of the thrust performance can be expected. In addition, depending on the laser power the laser-induced plasma occurring from a solid-propellant usually has a directed initial velocity, which can also improve the thrust performance compared to pure PPTs. In this study, a preliminary investigation was conducted on characteristics of pulsed discharges induced by laser pulse irradiation for various voltages applied to electrodes and on thrust performances for the laser-electric hybrid propulsion system of this type.

2. Experimental

2.1. Laser assisted PPT

A schematic of a laser-assisted plasma thruster developed in this study is illustrated in Fig.1⁵⁻⁶. The thruster utilizes a laser-beam assistance to induce a plasma region, ionized from a solid-propellant between electrodes, and then an electric discharge is induced in this conductive region. Since the plasma is induced through laser ablation of the solid propellant in this system, various substances, such as metals, plastics, ceramics, etc., in various phases can be used for the propellant. Therefore, this system must be effective not only for space propulsion devices but also for plasma sources in material processing. In addition, since the plasma has a directed initial velocity through the laser ablation, it is expected that the thrust efficiency and propellant mass loss should be significantly improved. Preliminary tests on a rectangular type thruster inserting a solid propellant between electrodes, shown in Fig.1, was conducted⁵⁻⁶. For the thruster (Figs.1 and 2), copper electrodes (5 mm in width, 20 mm in length) and an alumina propellant (3 mm in height) were used.

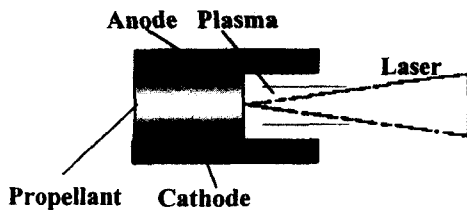


Fig.1 Schematic of a laser-assisted rectangular type PPT.

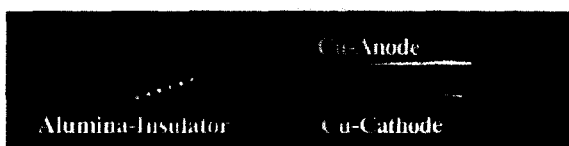


Fig.2 Photo of rectangular laser-assisted pulsed plasma thruster Channel length 20mm

2.2. Plasma behavior observation

A schematic of experimental setup is shown in Fig.3. A Q-sw Nd:YAG laser (BMI, 5022DNS10, wavelength: $\lambda=1064\text{nm}$, fixed pulse energy: 266 mJ/pulse, pulse width: 10 nsec) was used for a plasma source, or a laser assistance. The laser pulse was irradiated into a vacuum chamber (10^{-3} Pa) through a quartz window and focused on a target, or a propellant, with a focusing lens ($f = 100$ mm). Discharge current was monitored with a current monitor (Pearson Electronics, Model-7355, maximum current: 10 kA, minimum rise time: 5 nsec) and an oscilloscope (LeCroy, 9374TM, range: 1 nsec/div \sim 5

msec/div). In this study, preliminary experiments on switching, or discharge between cathode and anode, and discharge current characteristics of the laser-induced plasma were conducted. At the first part of the experiment, lowered voltage conditions (~ 100 V) applied on the electrodes were selected to examine discharge current characteristics under a low current range (~ 100 A). In addition, discharge current characteristics for higher current cases, or higher voltages (~ 2000 V), were also investigated. In order to observe temporal behaviors of exhaust plasma plumes, ICCD camera observation (ANDER TECHNOLOGY, minimum gate width: 2 nsec) was conducted.

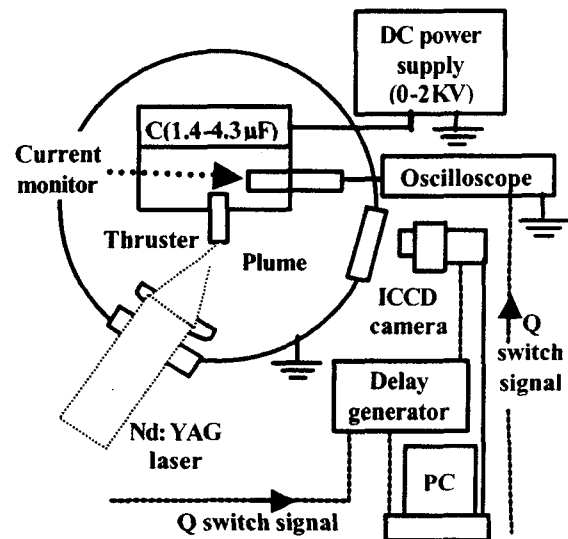


Fig.3 Schematic of experimental set up

Generating an arbitrary delay with a delay generator triggered by a Qsw output signal, the ICCD camera was synchronized with a laser pulse. Since this phenomenon was highly reproducible, it was possible to obtain images of a temporal growth of a plasma formation process with 2nsec resolution through changing the delay timing.

2.3. Thrust performance measurement

2.3.1. Thrust stand

In order to estimate μNsec -class impulses, a torsion-balance type thrust stand was developed and tested. A schematic illustration of the torsion-balance is given in Fig.4 and its photo is shown in Fig.5. The torsion-balance consists of a balance, a pivot, a displacement sensor, and a counter weight. The balance is 470 mm long made of aluminum. Distance between the pivot and thruster is set 350 mm. For the pivot, an aluminum C-section tube (450 mm in length, 6mm in outer diameter, 0.5 mm in thickness) was used⁷⁾. A torsional spring rate of the pivot estimated in this case is $k = 4.7 \times 10^{-2}$ Nm/rad⁷⁾. As for the displacement sensor, a Non-contacting displacement meter of eddy

current principle (EMIC, 503-F, NPA-010, maximum range: 1mm, minimum displacement: 0.5 μm) located at 344mm from the pivot was used. The counter weight consisting of brass plates was fixed at 70 mm from the pivot.

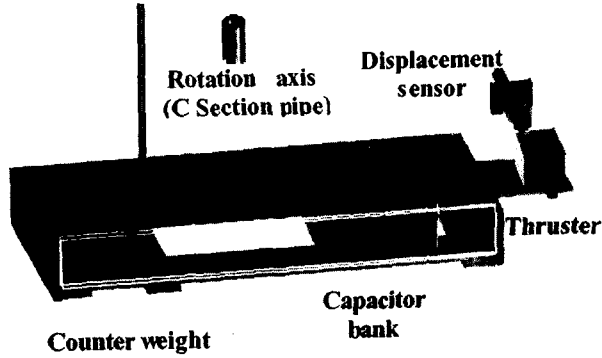


Fig.4 Schematic of a thrust stand

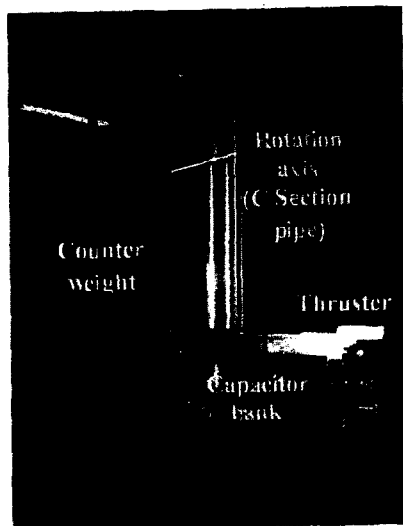


Fig.5 Photo of a thrust stand

2.3.2. Thrust estimation

An equation of motion of the balance is given as;

$$J \ddot{x} + \gamma \dot{x} + kx = I_m T(t) \quad (1)$$

, where I_m : distance from a pivot, x : displacement, $T(t)$: impulse,

$$\gamma_0 = \sqrt{\frac{k}{J}}, \quad (2)$$

k : spring rate, γ_0 : natural frequency, J : moment of inertia.

When an impulse $T(t) = I I_l \delta(t)$ acts on the balance at $t = 0$, a solution of Eq.(1) becomes as follows;

$$x(t) = A^* \sin \gamma_0 t \quad (3)$$

, where A^* : amplitude,

$$A^* = \frac{I I_l I_m}{J \gamma_0}, \quad (4)$$

, where I_l : impact point from a pivot.

If an amplitude A^*_{cal} is measured for a known impulse I_{cal} in calibration, an impulse can be estimated from a ratio of I_{cal}/A^*_{cal} , as follows;

$$I = \frac{J \gamma_0}{I_l I_m} A^* = \frac{I_{cal}}{A^*_{cal}} A^* \quad (5)$$

For different I_l and I_m cases in calibration,

$$A^*_{cal} = \frac{I_{cal} I_{mcal}}{J \gamma_0} \quad (6)$$

From Eq.(4), the impulse can be estimated as,

$$I = \frac{I_{cal} I_{mcal}}{I_l I_m} \frac{I_{cal}}{A^*_{cal}} A^* \quad (7)$$

2.3.3. Calibration

Calibration of the torsion-balance was conducted with known impulses using arbitrary impacts of an aluminum rod of 159 mg suspended by two strings of 480 mm in length. Velocities of the rod before and after the impacts on the balance were measured from images of a high-speed camera and an image-processing software. From the velocities, momentum changes, or the impulses, could be obtained.

The calibration was conducted not in a vacuum chamber but in a calibration room consisting of steel beams and plastic sheets isolating from influences of atmospheric convection.

A typical result is shown in Fig.6 A slope of the linear plots estimated by a least square method is 34.13 μNsec/V with $R^2 = 0.9965$. From Eq.(7), a calibrated value can be 36.29 μNsec/V.

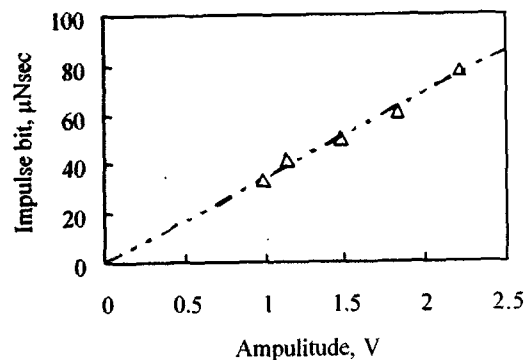


Fig.6. Result of calibration.

A schematic of an impulse measurement system is shown in Fig.7 and its photo in Fig.8. Two aluminum mirrors were used for optical alignment. Pulse energy of an incident laser beam was set 161 mJ.

Mass shots were estimated with an electronic-balance (SHIMADZU LIBROR AEX-200G) for cases of 266 shots and 401 shots with charged energy of 8.65 J. An average value of the mass shot is 1.026 μ g.

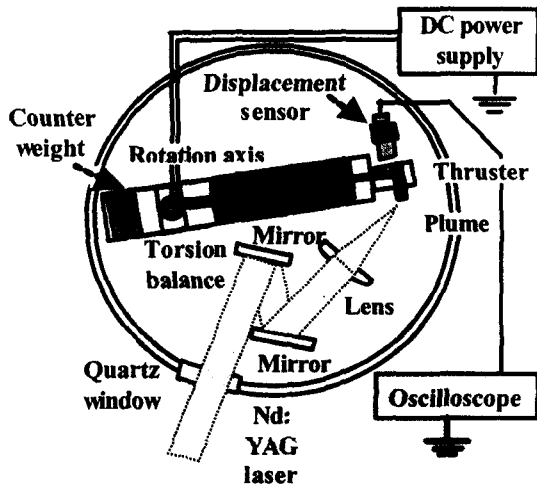


Fig.7 Schematic of experimental setup for measurement of an impulse bit.

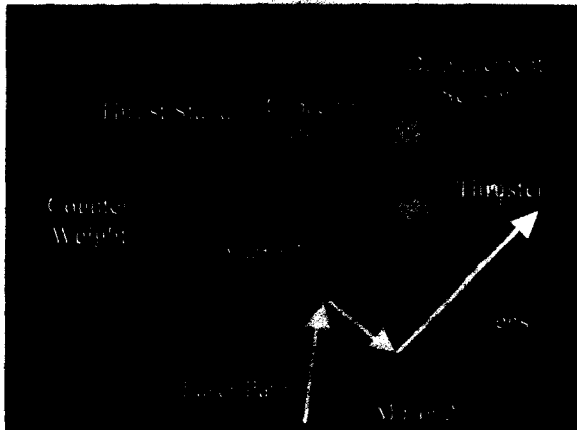


Fig.8 Photo of experimental set up for measurement of an impulse bit.

3. Results and Discussion

3.1 Discharge Characteristics and Plasma Plume Observation

Temporal variations of discharge current are given in Fig.9 for capacitors of 4.2 μ F. From the figure, the current, for example at 1000 V, abruptly rises and reaches a maximum value, 4000 A, at 1.5 μ sec, after which it falls down to a minimum value (-2000 A) at 4 μ sec and converges zero at about 18 μ sec. The current peaks are significantly higher in higher voltage cases. While with a higher capacitor case of 4.2 μ F, the peak current for a 2000V case is about 8000 A at 1.5 μ sec with its period of 6 μ sec. In this

case, estimated values of inductance and resistance were 212 nH and 57 m Ω , respectively.

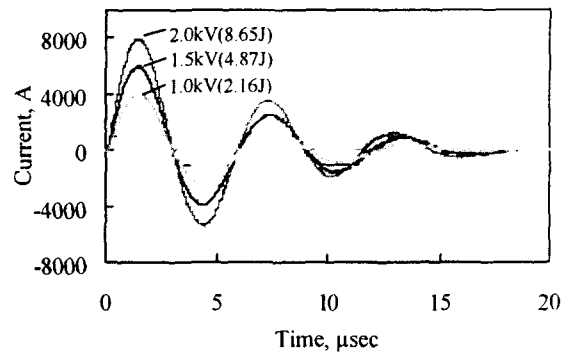


Fig.9 Temporal variations of discharge current of thrusters for high voltage and high capacity conditions.

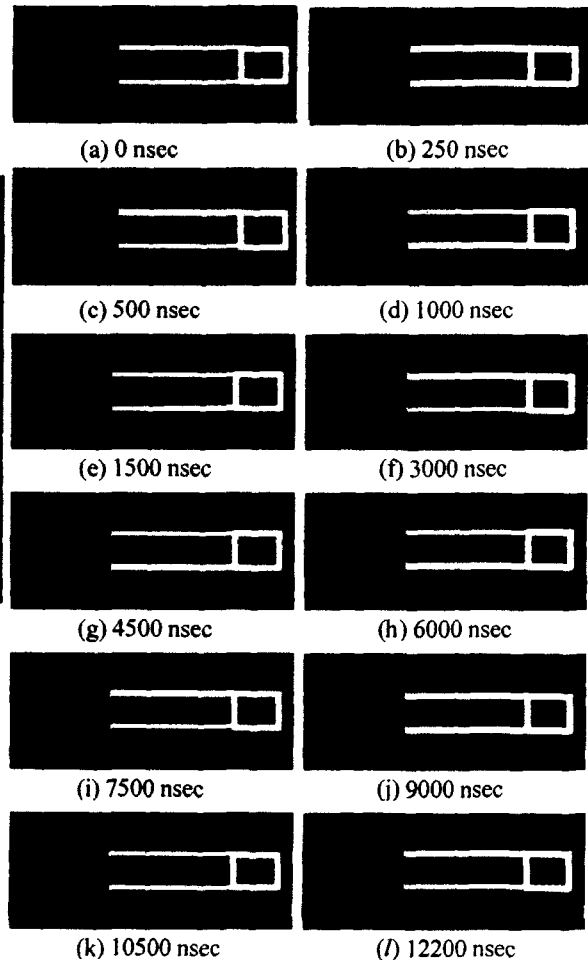


Fig.10 ICCD images of plume from a rectangular thruster (anode: upper plate) for 2000V.

ICCD camera images for charged energy of 2000 V are shown in Fig.10, in which larger capacitor of 4.2 μ F is employed to enhance an electromagnetic acceleration effect. A small spot plasma at the center

of an exposed propellant surface is induced after the laser irradiation. In this case, canted current sheet structures¹²⁾ can be seen from 1000 to 1500 nsec, where the current reaches the first positive peak as shown in Fig.9 and an associated electromagnetic effect probably becomes significant. Here, the plasma of anode side is moving faster than that of cathode side. Then the current reaches the first negative peak at 4500 nsec, in which the plasma of cathode side is faster than anode side, the second positive peak at 7500 nsec, and the second negative peak at 10500 nsec, as shown in Fig.6 for 2000 V. A laser-induced plasma is dominant up to 250 nsec. From these images of plasma emission distribution, velocity of the plasma through the laser ablation is estimated about 60 km/sec. Also, velocity of the current sheet is about 16 km/sec.

3.2 Thrust performance measurements

Plots of impulse bit measured with a torsion-balance type thrust stand for various energies charged to capacitors are shown in Fig.11. As shown in this figure, the impulse linearly increases from 3.36 to 38.1 μ Nsec with the energy up to 8.65 J. Although a value of about 5 μ Nsec is obtained even at 0 J, this is the case of the pure laser ablation with laser energy of 0.16 J.

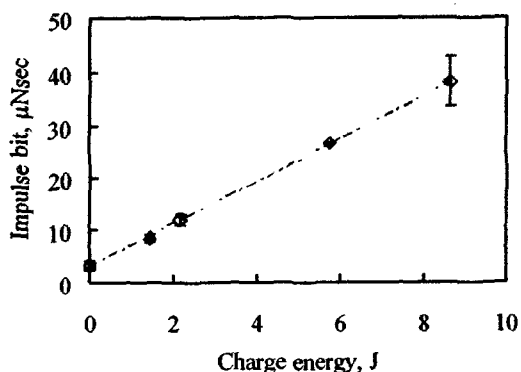


Fig. 11 Plots of measured impulse bit for various energies charged to capacitors.

Table 1 Mean values and standard deviations of measured impulses.

Charge energy, J	Amount of data	Impulse bit, μ Nsec	
		Mean value	Standard deviation
0	14	3.36	0.63
1.44	5	8.42	0.56
2.16	7	11.9	0.89
5.78	6	26.6	0.26
8.65	10	38.1	4.71

Mean values and standard deviations of the measured impulses are listed in Table 1. These

deviations are probably due to those of laser pulse energies and misalignments of mechanical and optical elements at each operation.

Relationship between momentum coupling coefficient and charged energy is shown in Fig.12. From the figure the coupling coefficient decreases with energy showing maximum value at 0 J, or in a pure laser ablation case. However, this maximum value is lower than those obtained in conventional laser ablation cases¹⁰⁾. This is probably because of a high ablation threshold of alumina influencing the low mass shot and high specific impulse.

Specific impulse variation with charged energy to capacitors are plotted in Fig.13. A linear increase of the specific impulse with energy can be seen in this figure. At 0, where pure laser ablation with laser energy of 0.16 J, specific impulse was about 300 sec. While in 8.65 J, $I_{sp} \sim 3800$ sec, which is significantly higher than conventional PPTs operated under similar energy levels. This is probably due to the directed initial plasma velocities, which is subsequently accelerated by an electromagnetic field, induced through the laser ablation in an initial phase.

Relationship between thrust efficiency ($=$ [kinetic energy]/[(charged energy) + (laser energy)] and charged energy are given in Fig.14. In these cases, laser pulse energy of 0.16 J was added to the charged energy in estimation of total energy (denominator).

As shown in this figure, thrust efficiency first decreases with energy from 0 to 1.4 J and then increases linearly with energy from 1.4 to 8.6 J. It should be noted in these cases that at a 0 J case, where pure laser ablation with laser energy of 0.16 J, thrust efficiency was higher than those of 1.4 J and 2.1 J cases. Therefore it was shown that the thrust efficiency could be lower than those of the pure laser ablation cases in low energy cases, in which contribution of electromagnetic effects on plasma acceleration was probably insignificant. In other words, thrust efficiency of the pure laser ablation thruster could be recovered with higher electric energy inputs.

Values of the thrust efficiency obtained in this study for input energy ranging 7 ~ 9 J are significantly higher than those of conventional PPTs³⁾. This is probably due to effects of directed initial velocity of the plasma induced through the laser ablation. Most portion of the plasma induced through laser ablation is supplied to a discharge channel as a propellant with directed initial velocity in a short duration (~ 700 nsec) before main discharge occurring at 1 ~ 1.5 μ sec, and leads the discharge. At the same time, most part of the plasma conducting a current is probably accelerated through an electromagnetic force or the Lorentz force. In this process, the late-time vaporization, which is related to one of primary losses in conventional PPTs, is insignificant. In addition, as shown in ICCD camera images in Fig.10, surface vaporization of a propellant surface through the primary discharge is not obviously occurring. This is

probably due to characteristics of the propellant, alumina, with high stability for heat and chemicals.

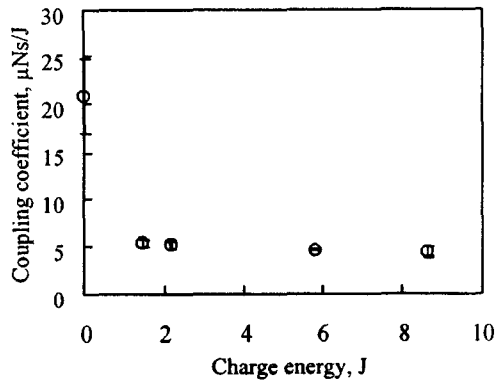


Fig.12 Plots of measured momentum coupling coefficient for various energies charged to capacitors.

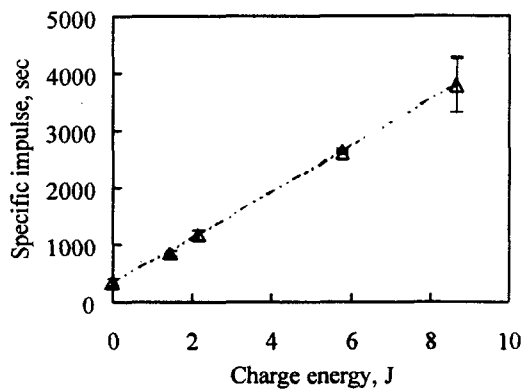


Fig.13 Plots of measured specific impulse for various energies charged to capacitors.

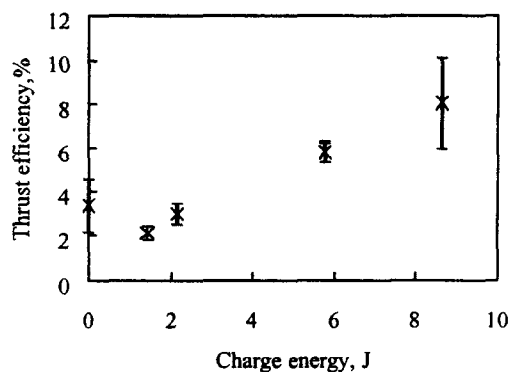


Fig.14 Plots of measured thrust efficiency for various energies charged to capacitors.

4. Conclusion

A fundamental study of newly developed rectangular laser-assisted pulsed-plasma thruster (PPT) was conducted. On discharge characteristics and thrust performances with increased peak current compared to our previous study to increase effects of electromagnetic forces on plasma acceleration. Following results were obtained.

- With 8.65 J discharge energy, maximum current reached about 8000 A.
- In plasma plume observation by ICCD camera at 8.65 J operation, current sheet structures could be seen.
- With a newly developed torsion-balance type thrust stand, thrust performances of laser assisted PPT could be estimated.
- The impulse bit and specific impulse linearly increased. On the other hand, coupling coefficient and the thrust efficiency did not increase linearly.. The coupling coefficient decrease with energy showing maximum value (20.8 $\mu\text{Nsec/J}$) at 0 J, or in a pure laser ablation cases. Thrust efficiency first decreases with energy from 0 to 1.4 J and then increased linearly with energy from 1.4 J to 8.6 J.
- At 8.65 J operation, impulse bit of 38.1 μNsec , specific impulse of 3791 s, thrust efficiency of 8 %, and coupling coefficient of 4.3 $\mu\text{Nsec/J}$ were obtained.

References

1. Jahn, R.G., *Physics of Electric Propulsion*: McGraw-Hill, 1968, pp.198-316.
2. Martinez-Sanchez, M., and Pollard, J. E., *J. Propulsion and Power* 14, pp.688-699 (1998).
3. Burton, R. L., and Turchi, P. J., *J. Propulsion and Power* 14, pp.716-699 (1998).
4. Micci, M. M., and Ketsdever, A. D. (ed.). *Micropropulsion for Small Spacecraft (Prog. Astronautics and Aeronautics 187)*: American Institute of Aeronautics and Astronautics, 2000, pp.337-377.
5. Horisawa, H., Kawakami, M., et al., *Beamed Energy Propulsion*: AIP Conference Proceedings Vol.664, 2003, pp.423-432.
6. Horisawa, H., Kawakami, M., et al., *IEPC 2003-75* (2003).
7. Masahiko Kameoka and Haruki Takegahara, Yukio Shimizu and Kyoichiro Toki., *IEPC2003-093* (2003).
8. H.,Koizumi, A,Kakami.Y,Furuta.,K,Komurasaki., and Arakawa.IEPC2003-087 (2003)
9. Markusic, T. E., and Choueiri, E. Y., *Proc. 26th IEPC*, pp.1196-1203 (1999).
- 10 Phipps, Jr, C. R., Turner, T. P., Harrison, R. F., York. G. W., Osborne, W. Z., Anderson, G. K., Corlis, X. F., Haynes, L. C., Steele, H. S., and Spicochi, K. C., *J. Applied. Phys.*, 64, pp.1083-1096 (1988).